Localized metabolic and t2 changes induced by voluntary and evoked contractions

Marc Jubeau, Yann Le Fur, Guillaume Duhamel, Jennifer Wegrzyk, Sylviane Confort-Gouny, Christophe Vilmen, Patrick J. Cozzone, Jean Pierre Mattei, Bendahan David, Julien Gondin

Localized Metabolic and T_2 Changes Induced by Voluntary and Evoked Contractions

MARC JUBEAU[1,2], YANN LE FUR[1], GUILLAUME DUHAMEL[1], JENNIFER WEGRZYK[1], SYLVIANE CONFORT-GOUNY[1], CHRISTOPHE VILMEN[1], PATRICK J. COZZONE[1], JEAN PIERRE MATTEI[1], DAVID BENDAHAN[1], and JULIEN GONDIN[1]

[1]Aix-Marseille Université, CNRS, CRMBM UMR 7339, Marseille, FRANCE; and [2]Laboratory "Motricité, Interactions, Performance", University of Nantes, Nantes, FRANCE

ABSTRACT

JUBEAU, M., Y. LE FUR, G. DUHAMEL, J. WEGRZYK, S. CONFORT-GOUNY, C. VILMEN, P. J. COZZONE, J. P. MATTEI, D. BENDAHAN, and J. GONDIN. Localized Metabolic and T_2 Changes Induced by Voluntary and Evoked Contractions. *Med. Sci. Sports Exerc.*, Vol. 47, No. 5, pp. 921–930, 2014. **Purpose**: This study compared the metabolic and activation changes induced by electrically evoked (neuromuscular electrical stimulation (NMES)) and voluntary (VOL) contractions performed at the same submaximal intensity using ^{31}P chemical shift imaging (CSI) and T_2 mapping investigations. **Methods**: Fifteen healthy subjects were asked to perform both NMES and VOL protocols with the knee extensors (i.e., 232 isometric contractions at 30% of maximal force) inside a 3-T scanner for two experimental sessions. During the first session, metabolic variations, *i.e.*, phosphocreatine (PCr), inorganic phosphate (Pi), and pH, were recorded using localized ^{31}P CSI. During a second session, T_2 maps of the knee extensors were obtained at rest and immediately after each exercise. Voxels of interest were selected from the directly stimulated *vastus lateralis* and from the nondirectly stimulated *rectus femoris*/*vastus intermedius* muscles. **Results**: PCr depletion recorded throughout the NMES session was significantly larger in the vastus lateralis as compared with the rectus femoris/vastus intermedius muscles for both conditions (VOL and NMES). A higher occurrence of Pi splitting and a greater acidosis was found during NMES as compared with VOL exercise, illustrating the heterogeneous activation of both slow and fast muscle fibers. T_2 changes were greater after NMES as compared with VOL for both muscles but were not necessarily related to the localized metabolic demand. **Conclusion**: We provided direct evidence that the metabolic demand was strongly related to both the exercise modality and the site of stimulation. On the basis of the occurrence of Pi splitting, we suggested that NMES can activate fast muscle fibers even at low force levels. **Key Words:** Pi SPLITTING, NEUROMUSCULAR ELECTRICAL STIMULATION, MOTOR UNIT RECRUITMENT, QUADRICEPS, ACIDOSIS

Neuromuscular electrical stimulation (NMES) involves the application of stimuli delivered as intermittent trains through surface electrodes usually positioned over the skeletal muscle belly to produce muscle contractions. The recruitment of motor units during NMES is largely different from that occurring during voluntary (VOL) contractions; that is, it is spatially fixed, temporally synchronous, nonselective, and mainly superficial; that is, close to the stimulating electrodes, allowing the activation of both slow and fast fibers at relatively low force levels (12,15).

A main limitation of this specific motor unit recruitment associated with NMES is an exaggerated metabolic demand (42,43), resulting in an earlier and greater muscle fatigue as compared with VOL at a given force level (16,25). For instance, two ^{31}P magnetic resonance spectroscopy (MRS) studies (42,43) demonstrated that NMES induced a larger phosphocreatine (PCr) depletion and acidosis as compared with VOL contractions performed at the same relative force output (42,43). For example, Vanderthommen et al. (42) reported a triphasic PCr time-dependent change during NMES exercise with an initial rapid drop followed by a steady-state and a paradoxical PCr resynthesis at the end of the stimulation protocol. However, the small diameter of the surface coil and the nonlocalized acquisition scheme used in their study restricted the metabolic investigations to superficial muscle areas, whereas deeper muscle fibers must have been activated due to the fact that the stimulation intensity was consistently increased during the NMES protocol (1). On that basis, the fatigue phenomenon occurring in the superficial muscle areas might account for the reported paradoxical PCr resynthesis, whereas the newly activated deeper muscle fibers did not contribute to the recorded metabolic variations. Overall, this necessarily led to an underestimation of the NMES-induced metabolic changes. Localized exercise-induced metabolic changes would then be of interest to accurately compare the already reported heterogeneous metabolic demand between NMES and VOL conditions (42,43).

Address for correspondence: Julien Gondin, Ph.D., Centre de Résonance Magnétique Biologique et Médicale (CRMBM), UMR CNRS 7339—Faculté de Médecine de la Timone, 27, Bd J. Moulin, 13005 Marseille, France; E-mail: julien.gondin@univ-amu.fr.
Submitted for publication February 2014.
Accepted for publication August 2014.

0195-9131/14/4705-0921/0
MEDICINE & SCIENCE IN SPORTS & EXERCISE®

DOI: 10.1249/MSS.0000000000000491

The emergence of high-field whole-body magnetic resonance (MR) scanners (i.e., ≥3 T) offers an interesting opportunity of acquiring spatially resolved ^{31}P data in exercising muscle using single-voxel MRS (28), direct PCr imaging (11,33), or ^{31}P chemical shift imaging (CSI) (4,10). Although this latter technique is typically associated with relatively long time resolution, it allows simultaneous metabolic recordings from different regions of interest including both superficial and deep muscle fibers. On that basis, ^{31}P CSI appears as a method of choice for an accurate comparison of the metabolic demand between VOL and NMES exercises. Moreover, ^{31}P CSI provides metabolic information not only from muscle areas close to the stimulating electrodes (i.e., directly stimulated) but also from those located outside the stimulated region (i.e., nondirectly stimulated). Finally, although splitting of the inorganic phosphate (Pi) peak has been previously reported (30,32,45) the exact underlying phenomenon is still debated. It has been put forward that Pi splitting might be related to the heterogeneous activation of different muscle fibers or different muscle groups (30,34,39). Due to the specific motor unit recruitment associated with NMES, one could hypothesize that ^{31}P CSI investigations could illustrate greater occurrence of Pi peak splitting during NMES as compared with VOL exercise.

MR imaging (MRI) T_2 mapping has been acknowledged as a relevant tool illustrating muscle activation (8,26). The T_2 increase in exercising muscle has been related to several factors including osmotically driven fluid shifts, metabolite accumulation, changes in intracellular pH, and altered perfusion/oxygenation (2,9,35,38). Interestingly, Adams et al. (1) reported a significant T_2 increase as a result of NMES contractions of different intensities, whereas T_2 changes were minor during VOL contractions of the same intensity. The authors suggested that the larger T_2 changes induced by NMES were related to a higher metabolic demand. By combining ^{31}P CSI and T_2 mapping, it has however been recently reported that muscles of the quadriceps with the greatest T_2 changes were not necessarily those presenting the greatest changes in PCr, Pi, or pH at least during a voluntary exercise (4). By using the same methodology (i.e., ^{31}P CSI and T_2), the comparison between voluntary and electrically evoked contractions would provide additional insights into the relation between metabolic demand and apparent muscle activity.

The purpose of the present study was first to localize the metabolic changes resulting from NMES and VOL contractions performed at a similar submaximal isometric force level. We hypothesized that a larger metabolic demand and a higher occurrence of Pi peak splitting would occur in the directly stimulated muscles as compared with VOL and the nondirectly stimulated muscles. We then combined ^{31}P CSI and T_2 mapping to further highlight the comparative analysis between the metabolic demand (as illustrated by ^{31}P CSI) and muscle activation (as illustrated by T_2 mapping).

METHODS

Subjects

Fifteen healthy male subjects (age, 28 ± 6 yr; height, 178 ± 4 cm; body weight, 68 ± 6 kg (mean ± SD)) devoid of neuromuscular injuries or disease participated in this study. Subjects were fully informed of the procedure and risks involved and gave their written consent. They were asked to refrain from physical exercise 2 d before the testing sessions. The experimental design of the study was approved by the Ethical Committee of "SUD MEDITERRANEE V" (reference: CPP 10.059), and the experiments were conducted in accordance with the Helsinki Declaration.

Study Design

Each subject participated in two sets of experiments performed inside a 3-T whole-body magnet (Siemens Verio MR system; Siemens AG, Erlangen, Germany). The two experimental sessions (duration, 90 min) were separated by at least 7 d and were performed at the same time of the day. For both experiments, subjects performed the VOL exercise (232 intermittent isometric contractions of the knee extensors, 750 ms on–750 ms off) with one leg and the NMES exercise (identical timing to the VOL exercise) with the contralateral leg. The first experiment was dedicated to ^{31}P CSI investigation of the metabolic changes induced by a standardized rest–exercise (i.e., NMES or VOL)–recovery protocol with 6, 8, and 10 CSI maps acquired (total acquisition time: 17 min and 24 s), respectively. The pattern of muscle activation was assessed for each exercise modality using T_2 mapping during the second experiment (experiment B) by acquiring T_2-weighted images at rest and immediately after each exercise (i.e., NMES or VOL). The order of the exercise (NMES vs VOL) and the involved leg were randomized and counterbalanced among the subjects. At least 3 d before data collection, subjects participated in a familiarization session to acquaint themselves with the NMES exercise. During the familiarization session, maximal voluntary isometric (MVC) force for both legs was determined for each subject after an approximately 5- to 10-min warm-up period including submaximal voluntary contractions (ranging from 10% to 75% of MVC).

Exercise

For both experiments, subjects were prone within the magnet with the foot attached to a home-made ergometer (20) equipped with a strain gauge (N2A-13-T026P-350; Vishay Micro-Measurements; Vishay Precision Group, Wendell, NC) to measure the force output during exercise. To avoid movement and/or contraction of other muscles than the quadriceps during exercise, subjects were firmly attached to the bed of the magnet with three nonelastic straps positioned over the leg, the hip, and the back. A noncompliant strap was also used to firmly attach the foot of

the subjects to the horizontal bars of the ergometer. The knee angle was set at approximately 40° (0° full knee extension). The force signal was amplified using a custom-made device, analog-to-digitally converted (PCI-6023E; National Instruments, Nanterre, France), and recorded on a computer (winATS software 6.5; SYSMA, Aix-en-Provence, France).

For the VOL exercise, subjects were asked to perform 232 isometric contractions (750 ms on–750 ms off) of the knee extensor muscles at approximately 30% of their MVC force. Real-time visual and auditive feedbacks were provided to the subject to reach the target force level and to gate the recordings of MR spectra during the 750-ms resting period.

The NMES exercise was identical to the VOL (i.e., in terms of contraction number and duty cycle) except that contractions were electrically evoked at a stimulation frequency of 30 Hz (500-μs pulse duration) using a commercially available stimulator (Digitimer DS7A; Digitimer Ltd, Hertfordshire, United Kingdom) interfaced with a train generator (Digitimer DG2A, Digitimer Ltd). A large self-adhesive electrode (5 × 13 cm; STIMEX, Rouffach, France) was placed over the *vastus lateralis* (VL) and *vastus medialis* (VM) muscles at 4 cm from the upper border of the patella. The second electrode (self-adhesive electrode 5 × 13 cm, STIMEX) was positioned on the proximal portion of the quadriceps muscle, i.e., at the insertion of the quadriceps. The two electrodes were separated by at least 25 cm, corresponding to the length of the dual tuned ^{31}P–^{1}H surface coil (see below). The electrode placement has been marked on the skin with semipermanent ink allowing an exact repositioning for the experiment B. The stimulation intensity was gradually increased throughout the NMES protocol to reach the target force level (i.e., 30% MVC). During experiment B, both the electrode placement and the stimulation intensity used for experiment A were replicated. For both experiments, subjects were instructed to relax during NMES.

MR Measurements

Experiment A. ^{31}P CSI was used to record the metabolic variations throughout a standardized rest–exercise (i.e., NMES or VOL)–recovery protocol with 6, 8, and 10 CSI maps acquired, respectively. Before the ^{31}P CSI acquisitions, the magnetic field homogeneity was optimized using a shim adjustment based on gradient echo double echo acquisition. A commercially available dual tuned ^{31}P–^{1}H surface coil (^{31}P: 18-cm-diameter loop, ^{1}H: concentric 15-cm-diameter loop, O-XL-HL-030-00721 V03; RAPID Biomedical GmbH, Rimpar, Germany) was positioned under the exercising quadriceps muscle. Pilot studies demonstrated that stimulation artifacts induced by NMES inevitably led to a poor signal-to-noise ratio. As a consequence, the surface coil had to be positioned between the two stimulating electrodes for the NMES exercise. For the VOL exercise, the distal part of the coil was located at 9 cm from the upper border of the patella (i.e., to take into account the electrodes' width of 5 cm) so that the coil placement was strictly similar to the one used for NMES exercise.

The sequence parameters of the localized ^{31}P CSI were as follows: 8 × 8 matrix, field of view (FOV) = 20 × 20 cm^2, slice thickness (ST) = 8 cm, TR/TE = 1500/2.3 ms, number of excitation = 1, elliptical phase encoding, flip angle = 120°, and bandwidth = 3000 Hz. The total acquisition time was 17 min and 24 s, including 24 CSI maps, resulting in a time resolution of 43.5 s. Images from the quadriceps muscles were obtained using a gradient echo sequence (TR/TE = 250/5 ms, FOV = 20 × 20 cm^2, eight slices, ST = 10 mm) and were used for the selection of voxels of interest (see below).

Experiment B. A six-channel body matrix coil (Siemens, Erlangen, Germany) was positioned around the exercising quadriceps muscle. T_2-weighted images were acquired at rest and immediately after each exercise using a nine-shot segmented spin-echo (SE)-echo planar imaging (EPI) sequence. The following acquisition parameters were used: echo train length = 13, TR = 4800 ms, TEs = 20, 30, 40, 50, and 60 ms, FOV = 25 × 25 cm^2, 11 slices, ST = 10 mm, interslice gap = 5 mm, phase partial Fourier: 6/8, matrix = 192 × 192, flip angle = 90°, number of excitation = 1, total acquisition time: approximately 6 min. Fat was suppressed by a short tau inversion recovery module (TI = 230 ms). Slices were positioned using the same anatomical markers than those used for the ^{31}P CSI investigations (i.e., upper border of the patella) so that T_2 images covered the whole muscle areas for which metabolic variations were recorded, i.e., between the two stimulating electrodes. T_1-weighted high-resolution anatomical images were also acquired for anatomical references by using a SE sequence. The following parameters were used: TR/TE = 490/13 ms, ST = 10 mm, FOV = 25 × 25 cm^2, matrix = 576 × 576.

Data Analysis

Mechanical data. The peak force and the force time integral, i.e., the area under the force traces, of each contraction were analyzed on a computer using commercially available software (winATS 6.5, SYSMA, Aix-en-Provence, France). Then, the average peak force and the sum of the force time integral were calculated for each protocol.

MR measurements. ***Experiment A.*** The first CSI map was discarded from the analysis given that the spin magnetization equilibrium was not reached at this stage. We selected two voxels of interest on the CSI map. Each voxel (2.969 × 2.969 × 8 cm^3) was therefore analyzed as a cylinder area (Fig. 1). Except for the VL muscle, it was impossible to isolate each muscle separately (rectus femoris (RF), vastus intermedius (VI), and VM) due to both the ST (8 cm) and the size of the voxels. Indeed, the selection of a voxel of interest in the distal slice of the VM muscle leads to an overlap with the sartorius muscle. On that basis, we deliberately chose to select a voxel from a directly stimulated muscle; that is, VL muscle, and a nondirectly stimulated muscle;

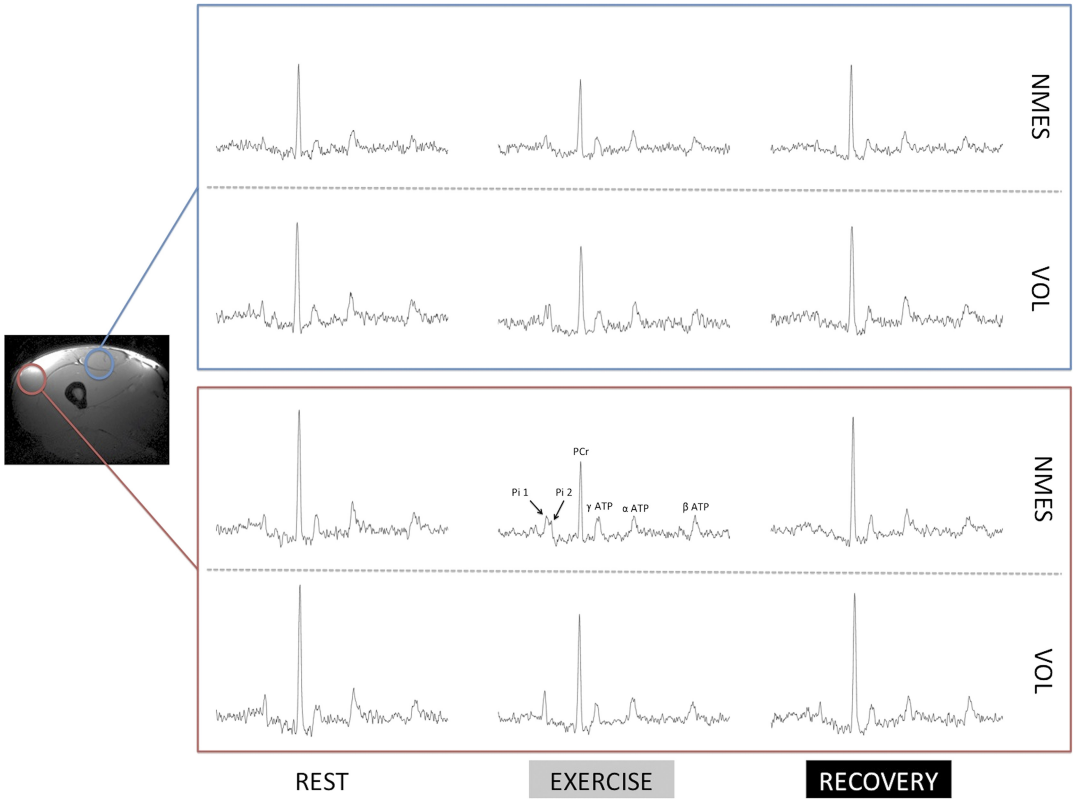

FIGURE 1—Representative anatomical images of the quadriceps muscle and spectra obtained by ^{31}P CSI before (REST), during (EXERCISE), and after (RECOVERY) electrically evoked (NMES) and voluntary (VOL) submaximal isometric contractions for the VL (red circle, bottom red subset) and RF/VI muscles (blue circle, top blue subset).

that is, including both the RF and VI muscle areas (Fig. 1). This latter voxel of interest therefore represents a mixture of the RF muscle; that is, superficial muscle and VI muscle, i.e., deep muscle (Fig. 1). Due to the limited number of encoding steps in CSI, a voxel contamination from neighboring voxels is unavoidable. We manually drew three regions of interest encompassing the VL, VM, and both the VI/RF muscles in which every point was took into account for the determination of voxel contamination. Within each region of interest, the MR signal was considered to be homogenous and a voxel of interest was positioned either in the VL or in the RF/VI muscles. The spatial response function (SRF), which indicates for a given pixel in the spectroscopic image the weight of contribution for all locations in the image (36), was centered in the corresponding voxel. It is well acknowledged that depending on how the positive and negative lobes of the SRF coincide with anatomical images, the signal contamination from adjacent regions can be additive or subtractive, so that the observed signal amplitude can change significantly. As a consequence, the SRF allowed us to determine how the surrounding area contaminated the voxel of interest. The analyses were performed on the second (i.e., distal), fourth (central), and sixth (proximal) slices for all the 15 subjects to consider the influence of the contiguous slices (i.e., through-plane effect). Measurements performed in 15 subjects showed that the average contamination was 9.3% ± 5.4% for VL and 9.4% ± 4.8% for RF/VI, without differences between slices. It should be pointed out that we consistently observed a high contribution to the VL signal of the region in close vicinity to the VI muscle. Nevertheless, our combined VI/RF voxel was deliberately positioned far from this region to avoid this contamination effect.

Relative concentrations of PCr, Pi, and adenosine triphosphate (ATP) were then obtained by a time-domain fitting routine using the *A*dvanced *M*ethod for *A*ccurate, *R*obust and *E*fficient *S*pectral fitting (AMARES) algorithm interfaced to in-house processing software (21). The mean of the five spectra recorded at rest was calculated and used for determining the concentrations of PCr and Pi, assuming an ATP resting concentration of 8.2 mM (17). Our time resolution (i.e., <45 s) was too low to accurately estimate the PCr recovery time with a monoexponential function given that this parameter typically ranges from 30 to 50 s for the quadriceps muscles (19). We therefore reported the time at which the PCr fully recovered; that is, when the PCr concentration was not significantly different to the baseline values. The same analysis was performed for pH values.

Intracellular pH was quantified from the chemical shift difference between the Pi and the PCr signals (31). To quantify Pi peak splitting in both conditions, a range of frequency (relative to PCr) was determined in the prior knowledge of the fit to distinguish the first peak (i.e., Pi 1, search range, 70–200 Hz) and the second peak of Pi (i.e.,

Pi 2, search range, 30–170 Hz). When two Pi peaks were present, the averaged pH value was calculated. During the postexercise recovery period, two consecutive spectra were summed to improve the signal-to-noise ratio and to allow a more accurate pH measurement.

Experiment B. Data processing was performed using an in-house program developed with Interactive Data Language (RSI, Boulder, CO). Quantitative T_2 maps were generated by fitting on a pixel-by-pixel basis the logarithm of the data to the following linear equation: $\log(S(\mathrm{TE})) = \log(S_0) - (\mathrm{TE}/T_2)$, where $S(\mathrm{TE})$ is the signal at time = TE and S_0 is the equilibrium magnetization. Mean T_2 values for the RF, VL, and VI muscles were determined before and immediately after each exercise by manually outlining regions of interest using a custom-written image analysis program. These measurements were done and averaged for all 11 slices.

Statistical Analysis

The reported values are presented as means ± SD except for figures for which SE values are presented for the sake of clarity. Distribution normality and variances homogeneity of the main variables were confirmed using a Skewness–Kurtosis normality test and the Levene's test, respectively. MVC force, relative force level, and force–time integral for both protocols (i.e., VOL and NMES) were compared using paired Student's *t*-tests. Changes in PCr concentrations, Pi, and pH were assessed using a two-way ANOVA (exercise–time) with repeated measures on time. A three-way ANOVA with repeated measures was used to compare T_2 measurements (exercise–muscle–time) between both protocols (VOL and NMES) and muscles (RF, VL, and VI) before and after exercise. A two-way ANOVA (exercise–muscle) was performed to compare the maximal PCr depletion between both conditions (VOL and NMES) and muscles (RF/VI and VL). A one-way ANOVA with repeated measures on time was also used to evaluate the changes in stimulation intensity during the NMES exercise. When a main effect or a significant interaction was found, Tukey's HSD *post hoc* analysis was used. Relationships between selected parameters were determined by Pearson product correlation. Significance was accepted when $P < 0.05$.

RESULTS

Mechanical data. The mechanical data recorded during both the spectroscopic (experiment A) and imaging (experiment B) sessions were not different. The MVC force recorded before the NMES and the VOL protocols was 416.1 ± 69.9 and 419.0 ± 59.1 N, respectively. Similarly, the force level averaged throughout the 232 contractions was similar for the NMES (28% ± 4% MVC) and the VOL (29% ± 5% MVC) protocols resulting in identical force time integrals. During the NMES protocol, stimulation intensity was linearly increased from 38 ± 5 to 76 ± 12 mA ($P < 0.05$) to maintain the target force level.

Experiment A: metabolic data. Both exercise protocols led to a significant PCr consumption in the two selected muscles (Figs. 1 and 2). As illustrated in Figure 2A, PCr fell rapidly and continuously during the NMES of the VL muscle so that for almost each time point, the PCr consumption was larger than the corresponding changes recorded throughout the VOL protocol. At the end of the exercise, PCr depletion amounted to 67% ± 21% for the NMES protocol and was significantly smaller (27% ± 23%, $P < 0.05$) for the VOL protocol.

For the RF/VI muscles, as displayed in Figure 2B, the initial PCr depletion was faster for the VOL as compared with the NMES protocol (39% ± 20% and 23% ± 12% for VOL and NMES, respectively, 220 s after the onset of the exercise). However, the end-of-exercise PCr depletion was comparable for the NMES (44% ± 17%) and the VOL (47% ± 26%) protocols (Figs. 1 and 2B). With regard to the specific muscle demand, PCr depletion recorded throughout the NMES session was significantly larger ($P < 0.05$) in the VL as compared with the RF/VI muscles for both conditions (VOL and NMES). Interestingly, PCr concentrations recorded during the NMES exercise in the VL muscle were negatively correlated ($R^2 = 0.46$) with the stimulation intensity at the corresponding time point ($P < 0.05$) (Fig. 3). A

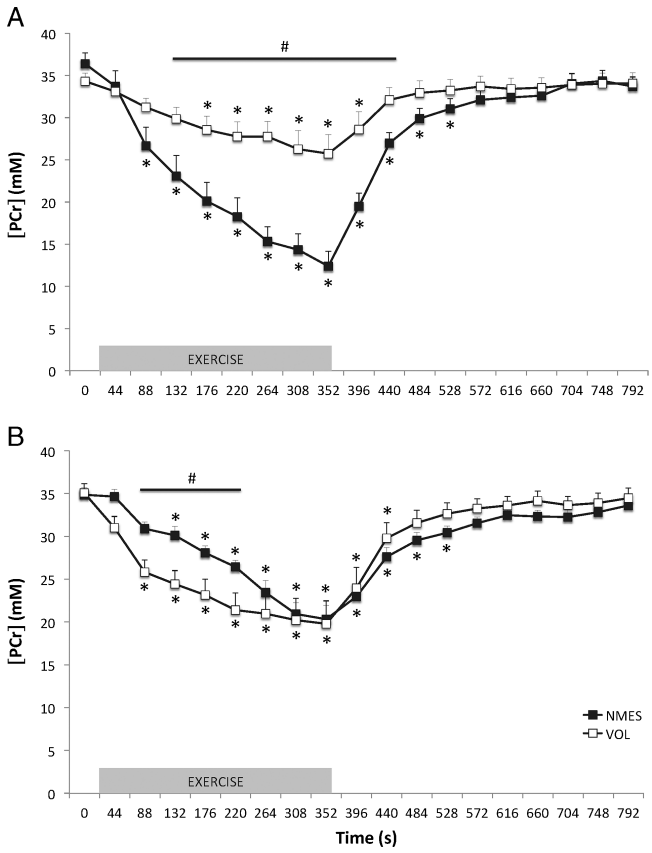

FIGURE 2—Absolute concentrations of PCr measured before, during (EXERCISE), and after electrically evoked (NMES) and voluntary (VOL) submaximal isometric contractions for the VL (traces A) and RF/VI muscles (RF/VI, traces B). Significantly different from baseline (i.e., time 0): *$P < 0.05$. Significantly different from VOL: #$P < 0.05$.

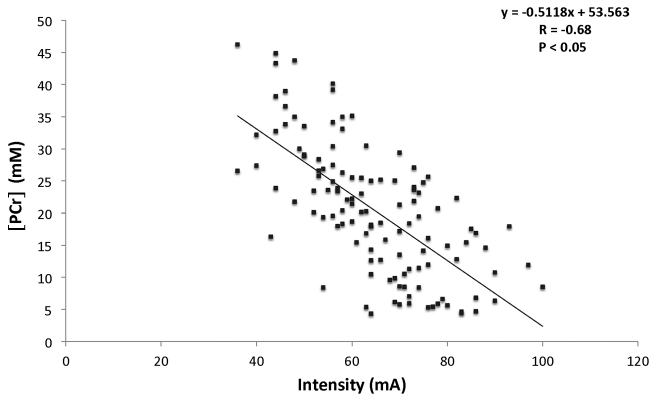

FIGURE 3—Relationships between PCr concentrations measured during exercise (EXERCISE), and the corresponding stimulation intensity during electrically evoked (NMES) exercise.

significant correlation between these two variables was also observed for the RF/VI muscles ($R^2 = 0.38$).

In the VL muscle, PCr was not significantly different to baseline values at 440 s after the onset of the VOL exercise, whereas it took longer (572 s) after the NMES exercise (Fig. 2A). For the RF/VI muscles, PCr concentrations returned to baseline values at 484 and 572 s for VOL and NMES protocols, respectively (Fig. 2B).

As expected, the total [Pi] time course evolved as a mirror of the [PCr] time-dependent changes (Fig. 4A–F). Indeed, total Pi significantly increased ($P < 0.05$) during both exercises and for both muscles (Fig. 1 and 4C, F). It is noteworthy that the Pi accumulation in the VL was significantly larger ($P < 0.05$) during NMES as compared with VOL protocol (Fig. 4C). Regarding the RF/VI muscles, total Pi was only significantly larger ($P < 0.05$) at the onset of the VOL exercise as compared with the NMES (Figs. 1 and 4F) due to the greater amplitude of the first peak of Pi (i.e., Pi 1) (Fig. 4D). However, similar values were reached at the end of the two exercises (Fig. 4F).

Interestingly, a splitted Pi peak was discernable in the VL of 13 subjects (out of 15 subjects) during the NMES protocol, whereas only two subjects displayed this phenomenon in the VL during the VOL protocol (Fig. 4A, B). Interestingly, the amplitude of the additional Pi signal (i.e., Pi 2) for the VL was also significantly higher ($P < 0.05$) for the NMES as compared with the VOL protocol (Fig. 4B). Although the occurrence of Pi splitting was also greater during NMES as compared with VOL in the RF/VI muscles (11 vs 8 subjects, respectively), no significant difference regarding the amplitude of the second Pi peak was observed for this muscle between both conditions (Fig. 4E). Overall, the contribution of Pi 2 to the total Pi was significantly greater ($P < 0.05$) during NMES as compared with VOL (Fig. 4B, E).

The extent of the end-of-exercise acidosis for the NMES protocol was significant, i.e., -0.28 ± 0.12 pH unit for the VL and -0.22 ± 0.11 pH unit for the RF/VI (Fig. 5). On the contrary, the intracellular pH remained constant throughout the VOL protocol for the VL (-0.05 ± 0.06 pH unit, Fig. 5A) ($P > 0.05$), whereas a slight decrease was measured for the RF/VI during VOL exercise (-0.14 ± 0.13 pH unit, Fig. 5B) ($P < 0.05$). The acidosis extent was then larger during the NMES than during the VOL exercise, regardless of the investigated muscles.

For the VL, pH values associated with the first peak of Pi (peak 1) and the second peak (peak 2) exercise were 6.90 ± 0.12 ($n = 15$) and 6.53 ± 0.10 ($n = 13$) during NMES and were 6.97 ± 0.05 ($n = 15$) and 6.79 ± 0.08 ($n = 2$) during VOL protocol, respectively. For the RF/VI muscles, pH values for peak 1 and peak 2 were 6.93 ± 0.07 ($n = 15$) and 6.54 ± 0.07 ($n = 11$) during NMES and were 6.95 ± 0.09 ($n = 15$) and 6.63 ± 0.08 ($n = 8$) during VOL, respectively.

During the recovery period of the NMES protocol, mean pH values were consistently lower ($P < 0.05$) than baseline values for the VL (Fig. 5A), whereas pH was not significantly different from baseline values after 792 s for the RF/VI muscles (Fig. 5B). After VOL exercise, mean pH values went back to baseline at 616 s (Fig. 5B).

Experiment B: muscle activation data. Quantitative MRI measurements showed that T_2 was significantly ($P < 0.05$) and similarly increased after NMES in all muscles: RF (+15% ± 12%), VL (+18% ± 14%), and VI (+14% ± 9%) (Fig. 6). On the contrary, T_2 only increased significantly ($P < 0.05$) in the RF muscle after the VOL protocol (+8% ± 6%). As a result, T_2 changes were greater ($P < 0.05$) after NMES as compared with VOL for all muscles (Fig. 6). Interestingly, the extent of the relative T_2 changes was negatively correlated to the pH value averaged over the recovery period ($R^2 = 0.38$) as well as to the maximal PCr depletion ($R^2 = 0.23$) and the Pi increase ($R^2 = 0.20$) during exercise.

DISCUSSION

To our knowledge, this is the first study comparing the metabolic and functional changes between NMES and VOL contractions of the knee extensors using ^{31}P chemical shift and T_2 imaging investigations. This combination of two different MR approaches allowed us to quantify the metabolic demand and to localize muscle activation in different muscle areas (i.e., directly vs nondirectly stimulated), including both superficial and deep muscle fibers. The major findings were that (i) the muscles directly stimulated by NMES had a greater metabolic demand and acidosis, as well as a greater occurrence of Pi peak splitting and T_2 changes as compared with voluntarily activated muscles for the same force output, (ii) the metabolic demand was strongly related to the site of stimulation during NMES, and (iii) T_2 changes were not necessarily related to the localized metabolic demand.

The larger PCr depletion we quantified during NMES as compared with voluntary contractions performed at the same intensity (i.e., 30% MVC) clearly indicates that the metabolic demand was higher during NMES as compared with VOL, a finding consistent with several previously reported studies (25,42,43). However, the NMES-induced PCr depletion in the present study was roughly linear, whereas Vanderthommen et al. (42) reported a triphasic PCr time-dependent

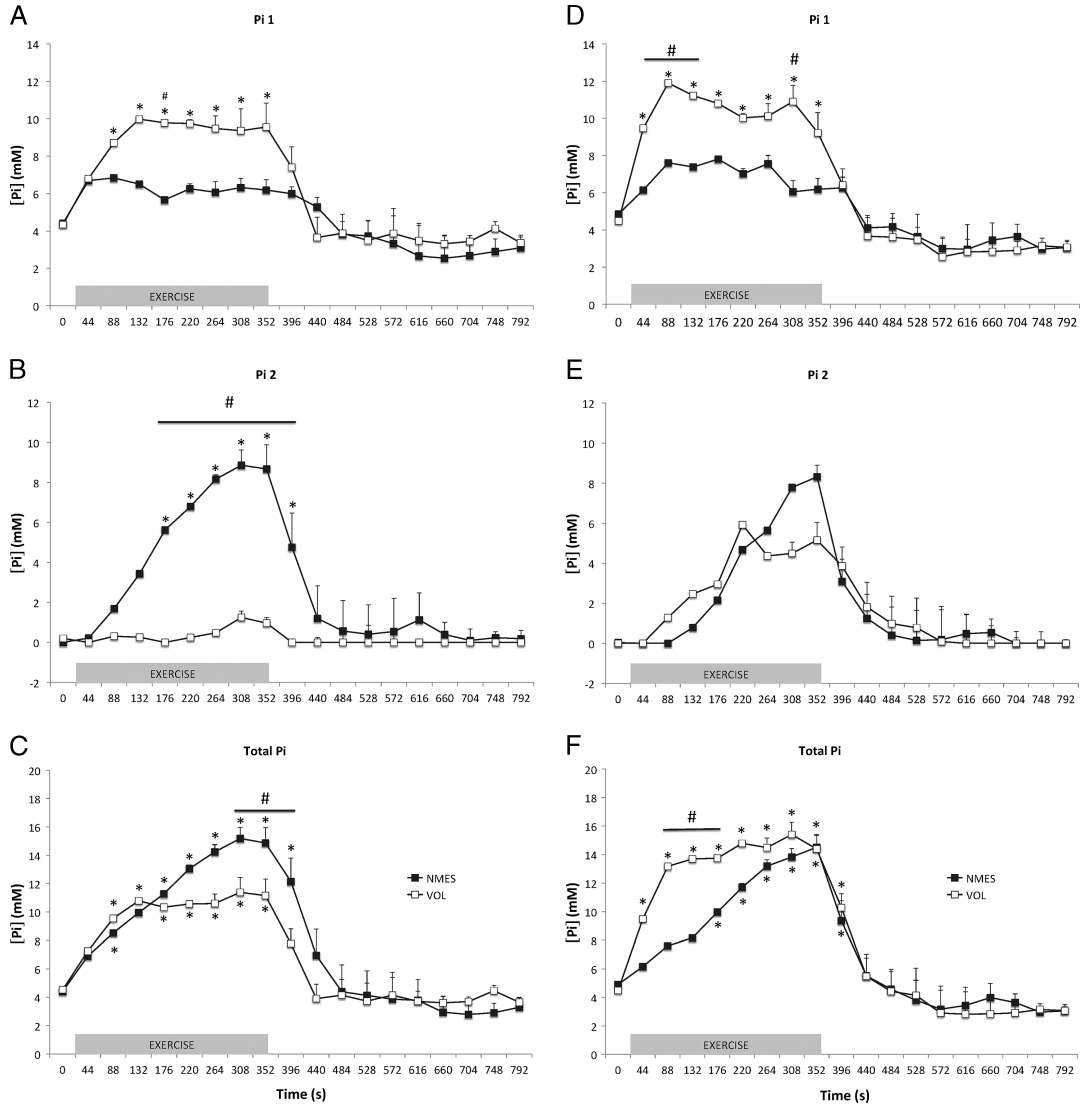

FIGURE 4—Absolute concentrations of the first peak (Pi 1), the second peak (Pi 2), and the sum of the two peaks (total Pi) of Pi measured before, during (EXERCISE), and after electrically evoked (NMES) and voluntary (VOL) submaximal isometric contractions for the VL (panels A, B, and C) and RF/VI muscles (panels D, E, and F). Significantly different from baseline (i.e., time 0): *$P < 0.05$. Significantly different from VOL: #$P < 0.05$.

changes with an initial rapid drop followed by a steady-state and a paradoxical PCr resynthesis at the end of the stimulation protocol. These differences might actually point out a number of methodological limitations in the latter study (nonlocalized acquisition technique and a small diameter of the surface coil), which led to an underestimation of the NMES-induced metabolic changes due to the noncontribution of deep muscle fibers to the recorded metabolic variations. On the contrary, the negative correlation we found between the stimulation intensity and the extent of PCr changes further illustrates that the higher the number of motor units recruited, the larger the metabolic demand as previously suggested (1) and clearly highlights the relevance of ^{31}P CSI investigation for an accurate monitoring of metabolic changes in exercising muscle. Overall, we reported for the first time the metabolic changes occurring in both initially and newly activated fibers during NMES.

The larger metabolic demand resulting from the NMES protocol was further illustrated by the lower recorded pH values as compared with those measured during VOL. Our findings are in accordance with those from Matheson et al. (24) illustrating significant intracellular acidosis from 7.15 to 6.6 after an 8-min NMES session. Likewise, Vanderthommen et al. (43) reported a significant pH drop as a result of NMES, whereas pH remained stable during VOL contractions. This larger acidosis recorded during NMES as compared with VOL likely illustrates a larger anaerobic contribution to energy consumption and/or a larger activation of fast fibers that have a greater ATP consumption (13). More interestingly, we consistently observed two Pi resonances during NMES likely reflecting an intracellular pH compartmentation. This Pi splitting has been previously ascribed to a simultaneous recruitment of oxidative and glycolytic fibers (30,34,39) and/or a sampling of

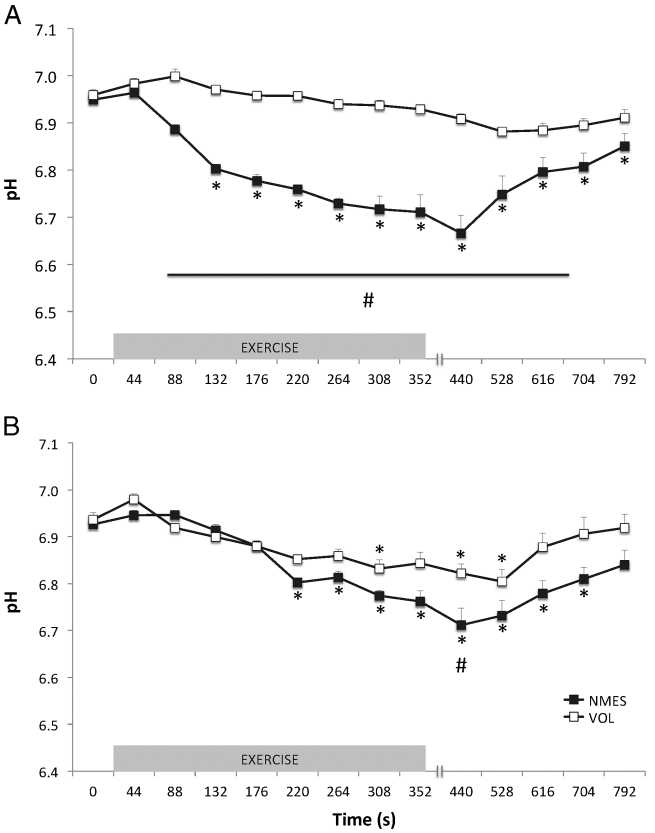

FIGURE 5—Mean pH measured before, during (EXERCISE), and after electrically evoked (NMES) and voluntary (VOL) submaximal isometric contractions for the VL (panel A) and RF/VI muscles (panel B). Significantly different from baseline (i.e., time 0): *$P < 0.05$. Significantly different from VOL: #$P < 0.05$.

both activated and nonactivated muscles (28) and/or to a reduced muscle perfusion (45). This latter hypothesis seems unlikely because a similar (18) or even an increased (41) muscle perfusion have been previously reported in response to electrically evoked contractions as compared with VOL protocol. One could largely assume that the higher occurrence of Pi splitting and the related greater acidosis during NMES as compared with VOL exercise illustrate the heterogeneous activation of both slow and fast muscle fibers. In the same way, the pH values associated to each Pi peak for the VL during NMES could be representative of two different populations of exercising muscle fibers (i.e., glycolytic and oxidative). These findings are in line with the specificity of the motor unit recruitment pattern during NMES, which is random/nonselective (12,15) compared with the orderly recruitment observed during voluntary contractions (i.e., size principle) (14). It is interesting to note here that during voluntary exercise at low force level (i.e., <30% MVC), mainly slow motor units are recruited. However, additional motor units (slow and fast motor units) can be recruited to maintain the torque level due to fatigue (i.e., alternate recruitment of motor units) (3,5), which might explain the occurrence of Pi splitting during VOL. Considering the low values of voxel contamination (i.e., approximately 10%), it seems unlikely that the sampling of both activated and nonactivated muscles can have significantly affected the Pi splitting we found in the present study. It should be pointed out that the use of even more accurate localized ^{31}P-MRS techniques (e.g., semi-LASER) at higher magnetic field (i.e., 7 T) (28,29), which are associated with negligible voxel contamination (i.e., approximately 1%), small voxel size (24–57 cm^3), and high temporal resolution (i.e., 6 s), would definitively provide relevant information about the physiological mechanisms accounting for the higher occurrence of two peaks of Pi associated with NMES. Overall, our ^{31}P CSI investigation suggests that NMES can activate fast muscle fibers even at low force levels (i.e., <30% MVC).

Although ^{31}P CSI investigation has been recently used for mapping the heterogeneity of the metabolic changes among voluntary activated muscles of the quadriceps (4), data were missing regarding electrically evoked contractions. We recorded, for the first time, the energy consumption occurring not only in the directly electrically stimulated VL muscle but also in the nondirectly stimulated RF/VI muscles. Interestingly, we observed both a larger PCr depletion and Pi accumulation in the directly stimulated VL muscle as compared with the nondirectly stimulated RF/VI muscles. Moreover, the earlier metabolic changes occurring in the directly stimulated muscle further confirm that motor axons close to the stimulating electrodes have been preferentially activated during NMES. On that basis, both superficial and deep muscle fibers located far from the active electrodes can only be recruited if the stimulation intensity is increased, thereby potentially inducing discomfort and/or pain sensations. Considering that the metabolic demand is largely dependent on the site and the intensity of stimulation, our results clearly illustrated the usefulness of either moving the active electrodes or using multipad electrode configuration of NMES programs to maximize the metabolic stress and to minimize the discomfort (22,23,37). This is highly relevant for clinicians and sport scientists who are in charge to conceive successful NMES programs for physically active subjects and hypoactive patients.

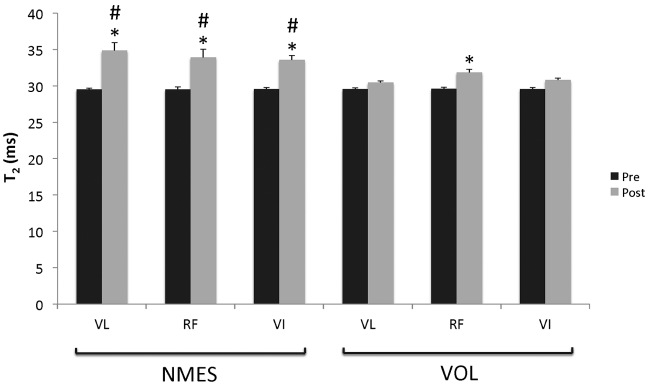

FIGURE 6—T_2 measured before (Pre) and after (Post) electrically evoked (NMES) and voluntary (VOL) submaximal isometric contractions for the VL, RF, and VI muscles. Significantly different from PRE: *$P < 0.05$. Significantly different from VOL: #$P < 0.05$.

In the present study, T_2 mapping was used as a measure of muscle activation as previously described (2,9,27,35,38) and combined to ^{31}P CSI to highlight the different response between metabolic demand and muscle activation. We demonstrated that T_2 changes were not necessarily related to the localized metabolic demand. Indeed, we quantified a larger PCr consumption and Pi accumulation in the directly as compared with the nondirectly stimulated muscles, whereas T_2 changes were similar for both muscles. Conversely, we observed larger T_2 changes in the RF and VI muscles during NMES than during VOL exercise despite similar energy consumption for both protocols. Although it has been recently proposed that intracellular metabolic accumulation and the resulting increase in intracellular water content could be the main determinant of postexercise T_2 changes (8), our results do not fully support this assumption. In line with our results, it has been recently reported that muscles of the quadriceps with the greatest T_2 changes were not necessarily those presenting the greatest changes in PCr, Pi, or pH after a voluntary exercise, suggesting a variability of the metabolic response across the active muscle groups (4). Although the linear relationship we reported between exercise-induced T_2 changes and maximal PCr depletion supports that changes in osmotically active metabolites might contribute, at least in part, to the exercise-induced T_2 changes, one could assume that other accounting factors such as acidosis, perfusion/oxygenation (2,9,35,38), and fiber-type recruitment could be involved. Indeed, we found a strong negative relationship between T_2 changes and the mean pH measured during recovery, a finding consistent with previous results in both humans and animals (7,40,44). However, considering that recovery kinetics of pH occurs within minutes although the corresponding T_2 recovery might last several hours (6,38), intracellular acidosis might not be the only accounting factor of T_2 changes. As previously mentioned, it should be pointed out that both an increased muscle perfusion (41) and a larger activation of fast muscle fibers (15) during NMES certainly contribute to the T_2 variations we observed. Thanks to the combination of ^{31}P CSI and T_2 mapping, our results further confirm that T_2 changes are multifactorial so that the estimation of the intensity of muscle recruitment/activation either between muscles or individuals on the sole basis of T_2 measurements may be biased.

In conclusion, this study provides direct evidence of the heterogeneous metabolic demand during NMES and voluntary contractions using a localized spectroscopy technique. The accurate recordings of metabolic variations of both initially and newly activated fibers during NMES indicated that the metabolic demand was strongly related to both the exercise modality (i.e., NMES vs VOL) and the site of stimulation. We also showed that T_2 changes were not necessarily related to the exercise-induced metabolic variations.

We thank Dr Virginie Callot for her helpful advice regarding MRI measurements and all the volunteers that participated in this study. This research was funded by the Association Française contre les Myopathies (AFM-TELETHON).

Author contributions are given as follows: significant manuscript writer, M. J. and J. G.; significant manuscript reviewer/reviser, M. J., Y. L. F., G. D., J. W., S. C. G., P. J. C., D. B., and J. G.; concept and design, M. J., C. V., P. J. C., J. P. M., D. B., and J. G.; data acquisition, M. J., C. V., J. W., S. C. G., and J. G.; data analysis and interpretation, M. J., Y. L. F., G. D., D. B., and J. G.; statistical expertise, M. J. and J. G.

No conflicts of interest, financial or otherwise, are declared by the authors. The results of the present study do not constitute endorsement by the American College of Sports Medicine.

REFERENCES

1. Adams GR, Harris RT, Woodard D, Dudley GA. Mapping of electrical muscle stimulation using MRI. *J Appl Physiol*. 1993; 74(2):532–7.
2. Bendahan D, Giannesini B, Cozzone PJ. Functional investigations of exercising muscle: a noninvasive magnetic resonance spectroscopy–magnetic resonance imaging approach. *Cell Mol Life Sci*. 2004;61(9): 1001–15.
3. Bickel CS, Gregory CM, Dean JC. Motor unit recruitment during neuromuscular electrical stimulation: a critical appraisal. *Eur J Appl Physiol*. 2011;111(10):2399–407.
4. Cannon DT, Howe FA, Whipp BJ, et al. Muscle metabolism and activation heterogeneity by combined 31P chemical shift and T2 imaging, and pulmonary O2 uptake during incremental knee-extensor exercise. *J Appl Physiol*. 2013;115(6):839–49.
5. Carpentier A, Duchateau J, Hainaut K. Motor unit behaviour and contractile changes during fatigue in the human first dorsal interosseous. *J Physiol*. 2001;534(Pt 3):903–12.
6. Cheng HA, Robergs RA, Letellier JP, Caprihan A, Icenogle MV, Haseler LJ. Changes in muscle proton transverse relaxation times and acidosis during exercise and recovery. *J Appl Physiol*. 1995; 79(4):1370–8.
7. Damon BM, Gregory CD, Hall KL, Stark HJ, Gulani V, Dawson MJ. Intracellular acidification and volume increases explain R(2) decreases in exercising muscle. *Magn Reson Med*. 2002;47(1):14–23.
8. Elder CP, Cook RN, Wilkens KL, Chance MA, Sanchez OA, Damon BM. A method for detecting the temporal sequence of muscle activation during cycling using MRI. *J Appl Physiol*. 2011;110(3):826–33.
9. Fisher MJ, Meyer RA, Adams GR, Foley JM, Potchen EJ. Direct relationship between proton T2 and exercise intensity in skeletal muscle MR images. *Invest Radiol*. 1990;25(5):480–5.
10. Forbes SC, Slade JM, Francis RM, Meyer RA. Comparison of oxidative capacity among leg muscles in humans using gated 31P 2-D chemical shift imaging. *NMR Biomed*. 2009;22(10): 1063–71.
11. Greenman RL, Wang X, Smithline HA. Simultaneous acquisition of phosphocreatine and inorganic phosphate images for Pi:PCr ratio mapping using a RARE sequence with chemically selective interleaving. *Magn Reson Imaging*. 2011;29(8):1138–44.
12. Gregory CM, Bickel CS. Recruitment patterns in human skeletal muscle during electrical stimulation. *Phys Ther*. 2005;85(4): 358–64.
13. Han YS, Geiger PC, Cody MJ, Macken RL, Sieck GC. ATP consumption rate per cross bridge depends on myosin heavy chain isoform. *J Appl Physiol*. 2003;94(6):2188–96.
14. Henneman E, Somjen G, Carpenter DO. Excitability and inhibitability of motoneurons of different sizes. *J Neurophysiol*. 1965; 28(3):599–620.

15. Jubeau M, Gondin J, Martin A, Sartorio A, Maffiuletti NA. Random motor unit activation by electrostimulation. *Int J Sports Med*. 2007;28(11):901–4.
16. Jubeau M, Sartorio A, Marinone PG, et al. Comparison between voluntary and stimulated contractions of the quadriceps femoris for growth hormone response and muscle damage. *J Appl Physiol*. 2008;104(1):75–81.
17. Kemp GJ, Meyerspeer M, Moser E. Absolute quantification of phosphorus metabolite concentrations in human muscle in vivo by 31P MRS: a quantitative review. *NMR Biomed*. 2007;20(6):555–65.
18. Kim CK, Strange S, Bangsbo J, Saltin B. Skeletal muscle perfusion in electrically induced dynamic exercise in humans. *Acta Physiol Scand*. 1995;153(3):279–87.
19. Layec G, Bringard A, Le Fur Y, et al. Comparative determination of energy production rates and mitochondrial function using different 31P MRS quantitative methods in sedentary and trained subjects. *NMR Biomed*. 2011;24(4):425–38.
20. Layec G, Bringard A, Vilmen C, et al. Accurate work-rate measurements during in vivo MRS studies of exercising human quadriceps. *MAGMA*. 2008;21(3):227–35.
21. Le Fur Y, Nicoli F, Guye M, Confort-Gouny S, Cozzone PJ, Kober F. Grid-free interactive and automated data processing for MR chemical shift imaging data. *MAGMA*. 2010;23(1):23–30.
22. Maffiuletti NA. Physiological and methodological considerations for the use of neuromuscular electrical stimulation. *Eur J Appl Physiol*. 2010;110(2):223–34.
23. Malesevic NM, Popovic Maneski LZ, Ilic V, et al. A multi-pad electrode based functional electrical stimulation system for restoration of grasp. *J Neuroeng Rehabil*. 2012;9: 66.
24. Matheson GO, McKenzie DC, Gheorghiu D, Ellinger DC, Quinney HA, Allen PS. 31P NMR of electrically stimulated rectus femoris muscle: an in vivo graded exercise model. *Magn Reson Med*. 1992;26(1):60–70.
25. McNeil CJ, Murray BJ, Rice CL. Differential changes in muscle oxygenation between voluntary and stimulated isometric fatigue of human dorsiflexors. *J Appl Physiol*. 2006;100(3):890–5.
26. Meyer RA, Prior BM. Functional magnetic resonance imaging of muscle. *Exerc Sport Sci Rev*. 2000;28(2):89–92.
27. Meyer RA, Prior BM, Siles RI, Wiseman RW. Contraction increases the T(2) of muscle in fresh water but not in marine invertebrates. *NMR Biomed*. 2001;14(3):199–203.
28. Meyerspeer M, Robinson S, Nabuurs CI, et al. Comparing localized and nonlocalized dynamic 31P magnetic resonance spectroscopy in exercising muscle at 7 T. *Magn Reson Med*. 2012;68(6):1713–23.
29. Meyerspeer M, Scheenen T, Schmid AI, Mandl T, Unger E, Moser E. Semi-LASER localized dynamic 31P magnetic resonance spectroscopy in exercising muscle at ultra-high magnetic field. *Magn Reson Med*. 2011;65(5):1207–15.
30. Mizuno M, Horn A, Secher NH, Quistorff B. Exercise-induced 31P-NMR metabolic response of human wrist flexor muscles during partial neuromuscular blockade. *Am J Physiol*. 1994;267(2 Pt 2):R408–14.
31. Moon RB, Richards JH. Determination of intracellular pH by 31P magnetic resonance. *J Biol Chem*. 1973;248(20):7276–8.
32. Moreno-Torres A, Rosset-Llobet J, Pujol J, Fabregas S, Gonzalez-de-Suso JM. Work-related pain in extrinsic finger extensor musculature of instrumentalists is associated with intracellular pH compartmentation during exercise. *PLoS One*. 2010;5(2):e9091.
33. Parasoglou P, Xia D, Chang G, Regatte RR. Dynamic three-dimensional imaging of phosphocreatine recovery kinetics in the human lower leg muscles at 3T and 7T: a preliminary study. *NMR Biomed*. 2013;26(3):348–56.
34. Park JH, Brown RL, Park CR, et al. Functional pools of oxidative and glycolytic fibers in human muscle observed by 31P magnetic resonance spectroscopy during exercise. *Proc Natl Acad Sci U S A*. 1987;84(24):8976–80.
35. Patten C, Meyer RA, Fleckenstein JL. T2 mapping of muscle. *Semin Musculoskelet Radiol*. 2003;7(4):297–305.
36. Pohmann R, von Kienlin M. Accurate phosphorus metabolite images of the human heart by 3D acquisition-weighted CSI. *Magn Reson Med*. 2001;45(5):817–26.
37. Popovic LZ, Malesevic NM. Muscle fatigue of quadriceps in paraplegics: comparison between single vs. multi-pad electrode surface stimulation. *Conf Proc IEEE Eng Med Biol Soc*. 2009;2009:6785–8.
38. Prior BM, Ploutz-Snyder LL, Cooper TG, Meyer RA. Fiber type and metabolic dependence of T2 increases in stimulated rat muscles. *J Appl Physiol*. 2001;90(2):615–23.
39. Vandenborne K, McCully K, Kakihira H, et al. Metabolic heterogeneity in human calf muscle during maximal exercise. *Proc Natl Acad Sci U S A*. 1991;88(13):5714–8.
40. Vandenborne K, Walter G, Ploutz-Snyder L, Dudley G, Elliott MA, De Meirleir K. Relationship between muscle T2* relaxation properties and metabolic state: a combined localized 31P-spectroscopy and 1H-imaging study. *Eur J Appl Physiol*. 2000;82(1–2):76–82.
41. Vanderthommen M, Depresseux JC, Bauvir P, et al. A positron emission tomography study of voluntarily and electrically contracted human quadriceps. *Muscle Nerve*. 1997;20(4):505–7.
42. Vanderthommen M, Duteil S, Wary C, et al. A comparison of voluntary and electrically induced contractions by interleaved 1H- and 31P-NMRS in humans. *J Appl Physiol*. 2003;94(3):1012–24.
43. Vanderthommen M, Gilles R, Carlier P, et al. Human muscle energetics during voluntary and electrically induced isometric contractions as measured by 31P NMR spectroscopy. *Int J Sports Med*. 1999;20(5):279–83.
44. Weidman ER, Charles HC, Negro-Vilar R, Sullivan MJ, MacFall JR. Muscle activity localization with 31P spectroscopy and calculated T2-weighted 1H images. *Invest Radiol*. 1991;26(4):309–16.
45. Yoshida T, Watari H. Effect of circulatory occlusion on human muscle metabolism during exercise and recovery. *Eur J Appl Physiol Occup Physiol*. 1997;75(3):200–5.